Advances in Science and Technology Research Journal

Advances in Science and Technology Research Journal, 2026, 20(8), 269–281
https://doi.org/10.12913/22998624/221467
ISSN 2299-8624, License CC-BY 4.0

Received: 2026.03.25
Accepted: 2026.06.01
Published: 2026.07.01

Experimental investigation and prediction of the tensile strength and surface roughness of fused deposition modeling-printed thermoplastic polyurethane parts using response surface methodology and artificial neural network models

Warqaa Majid Saeed[1], Abdullah Faraj Huayier[1], Alaa Hassan Shabeeb[1*]

[1] College of Production Engineering and Metallurgy, University of Technology, 10066 Baghdad, Iraq
* Corresponding author's e-mail: alaa.h.shabeeb@uotechnology.edu.iq

ABSTRACT

The versatility across engineering applications, low production costs, and environmental sustainability position 3D printing as one of the most promising manufacturing technologies. Process parameters directly govern the quality of printed parts, making their optimization essential for performance enhancement. This paper explores how tensile strength and surface roughness of FDM-printed parts of thermoplastic polyurethane (TPU) can be optimized and predicted using Taguchi, RSM and ANN models. Taguchi L27 orthogonal array design and ANOVA were used to test the effects of layer thickness (0.16, 0.2, 0.24 mm), infill density (40,60,80%), and infill pattern (Gyroid, Grid, Line) to achieve higher-the-better UTS and lower-the-better (Ra) per the ASTM D638 Type IV test. Optimal settings (LT 0.24 mm, ID 80%, IP Line) had a maximum UTS of 38.463 MPa, (LT 0.20 mm, ID 60, IP Grid) had a minimum RA of 1.88 µm, the infill pattern had the greatest effect on UTS (38.1 percent, p=0.043), and layer thickness had the greatest effect on RA (47.4 percent, p=0.010). The prediction was done using response surface methodology (RSM) and artificial neural network (ANN) model. ANN performed better than RSM with maximum prediction errors of 6.90 (UTS) and 6.49 (Ra) compared to the higher values of RSM, lower values of MSE, and an outstanding correlation coefficient of R = 0.99997. The validation of ANN on the experimental data indicated the high accuracy (MAE 0.011 UTS, 0.032 Ra) was achieved with the training of Levenberg-Marquardt (70-15-15 split), and the standard errors were low among all the runs. This combination of Taguchi design, RSM, ANOVA, and interpretable ANN modeling is a powerful scheme of optimization of the parameters of the FDM process when printing TPU, which improves the mechanical performance and the surface quality of the material in flexible engineering tasks.

Keywords: FDM, TPU, RSM, ANN, tensile strength, surface roughness.

INTRODUCTION

Additive manufacturing (AM), commonly referred to as 3D printing, enables the fabrication of diverse polymers and metals by building objects layer-by-layer from digital designs [1]. This approach delivers key economic benefits, including reduced prototyping expenses, accelerated production times, lower overall manufacturing costs, and minimized inventory needs. However, AM also presents technical limitations such as elevated operational expenses across varying conditions, comparatively slow deposition rates, and constraints on producing large-scale components. Its ability to produce intricate geometries with superior flexibility and cost-effectiveness has fueled widespread adoption in fields like architecture, automotive design, artistic endeavors, healthcare, and aerospace. Today, sectors including electronics, medicine, and aviation heavily rely on AM technologies [2].

Additive manufacturing techniques take various forms, such as laminated object manufacture (LOM), selective laser fusion (SLM), fused deposition modeling (FDM), plastic sheet

spinning (PSL), and finally, selective laser sintering (SLS) [3]. The use of polymers prevails in the industry in terms of the most widely used raw material for molding, which shows an immense level of efficiency [4]. The most preferred method, which is actually the most used technique, is the fused filament fabrication (FFF) or the three-dimensional printing (3DP) technique, which is called FDM [5]. The reasons for the higher level of usage could be the simplicity of the deposition method, the availability of the equipment, which are sold at a comparatively low price, and the readily accessible varieties of printing filaments that are available in the market [6].

The scientific community has been involved in researching and optimizing molten deposition modeling modelling process parameters for thermoplastic polyurethane and composites with improved mechanical properties and functionality. The factors which help in enhancing the shape memory properties of TPU were presented by Ameen et al. [7] at a temperature and velocity of 230 °C and 20mm/s with the highest compressive strength as 3.6082 MPa, and also presented by Yadavalli et al. [8], emphasizing that the pattern 'Gyroid' performed better than others regarding stress distribution. Jakab and Lendvai [9] proved that at the diameter of the nozzle and trast angle as 0.8mm and 0°, the highest value of tension strength is achieved, Salbiah et al. [10] demonstrated that RSM methodology was utilized for controlling the printing speed and temperature for improved functionality, and Albardawil et al. [11] – The "Taguchi" method for improving TPU95A functionality. Moreover, Elmrabet and Siegkas [12] demonstrated that filler ratio and size directly affected designs, and also, with conductive carbon and improved functionality by Kim [13], parts with pressure sensitivity were created for TPU. While considering the applications, Wang et al. [12] examined the shock-absorbing property for pneumatic tires, whereas Fallahiarezoudar et al. [14] produced the biomagnetic composites and Ferretti et al. [15] reviewed the printing of the biological organ to resemble human tissue. Conversely, Soykan [16] explored the influence of pigments on the crystallization process, Ursini and Collini [17] examined the behavior of lattice structures, and Haryńska et al. [18] synthesized porous structures for the engineering of bones. Rodríguez et al. closely focused on the parameters of dimensional accuracy and surface finish as the interaction of the influence of layer height and extrusion temperature to guarantee the accuracy of fabricated flexible materials [19]. On the other hand, Kumar et al. had an analysis on multi-material specimens of ABS-TPU made through laminated object manufacturing (LAM) and explored the microscopic properties of the combination strength and shape of different layers to guarantee the robustness under the influence of shearing stress conditions [20]. Through a comparative approach, Viccica et al. [21] tested the influence of an open and closed system in FDM technology, concluding that the management of ambient temperatures and dynamic values during printing is, in any case, fundamental to enhance material elongation and eliminate excessive stiffness. Lastly, Kulkarni et al. [22] examined on the feasibility of transforming TPU models into cellular ceramics. They tested the influence of the type of TPU material (polyester and polyether) and Shore hardness value (Shore A 80 and Shore A 90) on the success of the polyciliate impregnation and thermal decomposition process, demonstrating and confirming in their findings that the hardness value of the base material is fundamental in determining the material density and porosity of the resultant ceramic material, and thus, in turn, the key factor in ensuring the functional characteristics of the product.

This paper is devoted to the optimization of the FDM parameters, which is aimed at creating the TPU components concerning the overall optimization of the parameters in order to increase the strength and surface quality by predictive models. With a complex experimental design that requires three key parameters, including layer thickness (LT), infill density (ID), and infill pattern (IP), performance parameters were explored systematically. Tensile strength and surface roughness were studied in a total of 27 experimental runs. This paper uses RSM and ANN to examine the performance of TPU components and come up with the correct and dependable prediction models. This combined methodology can give a complete picture of how the parameters of FDM processes affect the quality of TPU parts, and this area will open the path to efficient and high-performance additive manufacturing.

METHODOLOGY

Material and method

The first step in the 3D printing process is the design of the part or component through design software. The CAD file is generated using the SOLIDWORKS program. The 3D model can be scaled into a common format after it is ready, and the most popular file format is the STL file format, as it is compatible with many other platforms and devices that are available in the market. This is then translated into the desired 3D printing language, G-Code typically on an FDM printer. This program shows the way the printer should move, become faster or slower, the desired printing temperature, built-in cooling mechanisms, and other processes. Figure 1 illustrates the sequence of work that the study will be guided by, where the selection of FDM parameters is considered as the starting point, and the percentage difference between the predicted and the measured values is taken as the final point. The Cura 4 was used to edit the STL file developed in SolidWorks. 13. 1, which also enables it to be readable by the machine to be used and 3D-printable. Figure 2 describe the solid model that was fabricated according to ASTM D638 Type 4.

The choice of process parameters also contributes significantly to the quality of the parts that are manufactured using FDM [23]. The parameters that were noticed in this research are the height of the layer, the density of infill, and the infill pattern. The change in such FDM environments has significant impacts on the process products, such as tensile strength and roughness on the surface [24]. In this way, the result of the general process

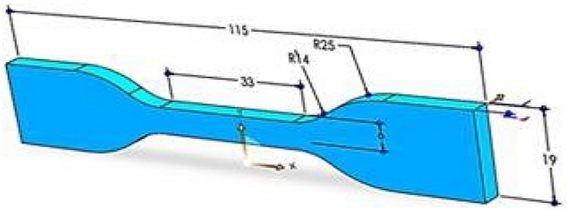

Figure 2. Tensile test specimen ASTM D638 Type 4

might be enhanced through the choice of the most appropriate FDM parameters [25]. Table 1 provides the process parameters that are selected, and their value to print the parts, and Table 2 contains other FDM parameters that did not vary during the course of the experiment. In this case, the experimental activities in this section of the study are elucidated in this section as illustrated in Figure 3.

The FDM parameter levels were chosen relying on the previous experience, extensive literature review, the importance of the main parameters determined in the course of initial experiments, and the high and low limits suggested by the manufacturer [26]. The three or more levels per parameter will offer a greater ability to capture the behavior of response variables. The Taguchi method was used to design experiments in which tensile tests are performed in accordance with the requirements of the ASTM D638 Type 4[27].

The Taguchi method uses signal-to-noise (S/N) ratios in order to measure the deviations when compared to the target levels of performance. It identifies the three types of characteristics, namely: nominal-the-best, higher-the-better, and lower-the-better [28]. This classification facilitates the parameter optimization towards the best system performance. In this case, tensile strength (higher-the-better) and surface roughness (lower-the-better) were the

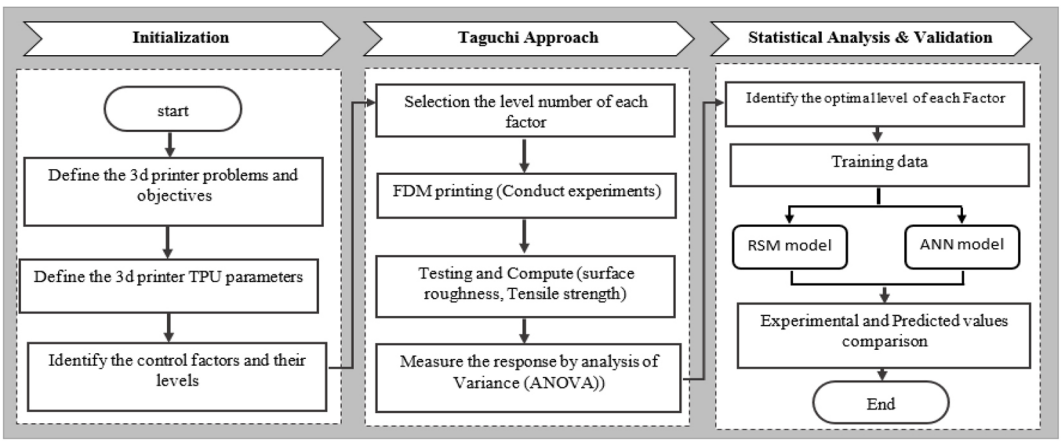

Figure 1. Methodology workflow

Table 1. Factors and their levels

FDM parameters	Units	Levels		
		1	2	3
Layer thickness (LT)	(mm)	0.16	0.2	0.24
Infill density (ID)	%	40	60	80
Infill pattern (IP)		Gyroid	Grid	Line

Table 2. Fixed parameters

Parameter type	Values	Units
Wall thickness	1.2	mm
Printing speed	55	mm/s
The temperature of the nozzle	225	Degree Celsius

objectives. S/N ratios of traits that are higher-the-better follow Equation 1, and the lower-the-better ratios follow Equation 2 [29].

- Larger is better:

$$S/N = -10\ log(\ 1\ n \sum 1\ yk\ 2\ n\ k{=}1\ ) \quad (1)$$

- Smaller is better:

$$S/N = -10\ log\ (\ 1\ n \sum 1\ yk\ 2\ n\ k{=}1\ ) \quad (2)$$

In which n is the number of tests, and yk is the value of the performance characteristic.

Tensile test using WDW200E computer-driven electronic universal testing machine was practiced as per ASTM D638 Type IV in order to get the mechanical properties of the specimens that were made. The tensile properties of the specimens are represented in Figure 3. The test was conducted at room temperature and with a steady crosshead speed of 1.5 mm/min. The experiment was used to capture three types of data: load, deformation, stroke, and time. Finally, the tensile strength was obtained with the help of peak loading values that were obtained in the same way, which were related to the true dimensions of specimens (and not to the parameters of their CAD models). These experimental results were subsequently used in calculating the values of stress and mechanical properties, and also estimating the tensile strength of both of the TPU test specimens as per Equation 3.

$$\sigma = F/A \quad (3)$$

where: σ – tensile stress (N/mm^2); F – applied force (N); A – cross section area (mm^2).

The roughness of the tensile test specimens was tested on a Pocket Surf profilometer (Figure 3). At each specimen, three measures were made at varying points, making sure that the roughness profile is not inclined to the orientation of the lay. Each measurement was used to calculate Ra, and

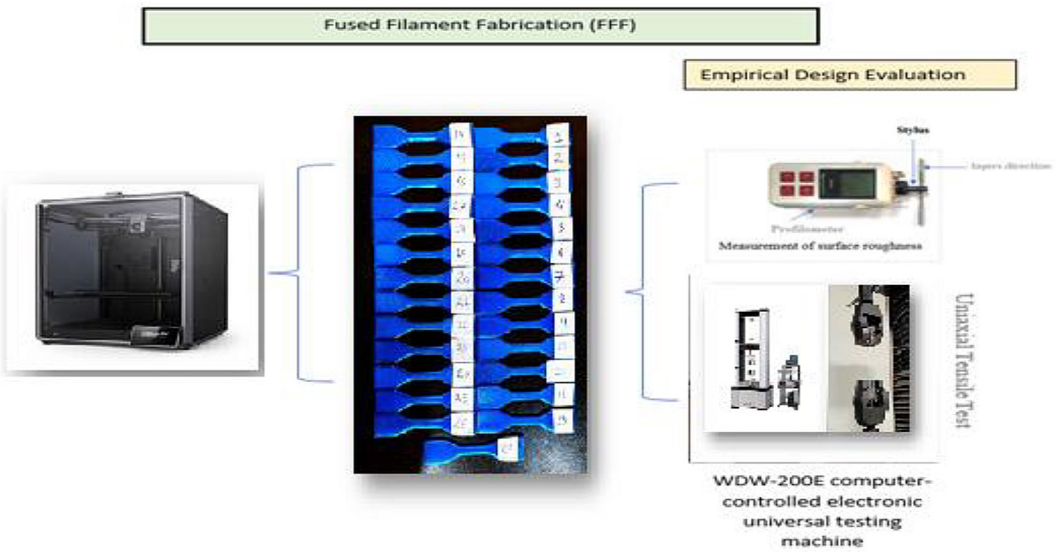

Figure3. Experimental workflow

the average of the three values was taken as the final surface roughness of the printed specimen.

Response surface methodology

Response surface methodology (RSM) is a statistical tool that aims at modelling and optimizing processes by seeking the interrelationship between various input variables and response outputs. It has a high accuracy in approximating complex response surfaces by empirical representation by use of polynomials, which is ideal in determining the best conditions in experimental designs. It is widely used in engineering optimization, and its nonlinear interaction mapping is an efficient way to explore the interactions with a relatively small number of experiments compared to one-factor-at-a-time methods [30]. RSM can display curvatures, interactions, and optima of a model without exhaustive testing by modeling the data with quadratic models [31]. The core of RSM is a second order, which is demonstrated in the Equation 4:

$$y = \beta_0 + \sum_{i=1}^{4} \beta_i X_i + \sum_{i=1}^{4} \sum_{j=1}^{4} \beta_{ij} X_i X_j + \\ + \sum_{i=1}^{4} \beta_{ii} X_i^2 \quad (4)$$

The RSM was applied in this work with the help of the MINITAB software that was used to determine the influence of the main 3D printing factors, such as layer thickness, infill density, and infill pattern, on the tensile strength and roughness of printed specimens. The experimental design was based on Box-Behnken matrices, so that response surface models could be developed using the data effectively. RSM was capable of successful modelling of the nonlinear interaction between printing parameters and mechanical properties, providing useful information about process optimization [32]. This method underscores how versatile and strong RSM is in the field of engineering to be used as a potent predictive modeling and decision-making tool [33].

Artificial neural network

An artificial neural network (ANN) is a computational model that is based on biological neural networks of the human brain [34]. It is a network of interlinked nodes or neurons arranged in an input layer, one or more hidden layers, and an output layer [35]. The information is being passed over the network, and connection weights are modified with training. The input data is fed repeatedly, and weights are adjusted according to the difference between the predicted and the actual output. The ANN model in this study will have three input neurons (layer height, infill density, and infill pattern) with an input matrix of (3 × 27) and two output neurons (tensile strength and surface roughness) with an output matrix of (2 × 27). The training is determined by the Hebbian learning rule. Hebbian learning was particularly selected as it was able to embody local associations between neighboring printing conditions and mechanical output feedbacks (tensile strength and surface roughness) [36]. The neural fitting tool was used to process these inputs and outputs depicted in Figure 4. The research also used ANNs to simulate the nonlinear connections among 3D printing parameters and material properties to obtain important data regarding the optimization of the processes [37]. This approach highlights the versatility and stability of ANNs in the field of engineering, making them a useful instrument of predictive modeling and informed decision-making.

RESULTS AND DISCUSSION

Analysis the results

Table 3 gives the measured tensile strength and the surface roughness of 27 FDM-printed specimens after printing. The experimental data were subjected to MINITAB software to

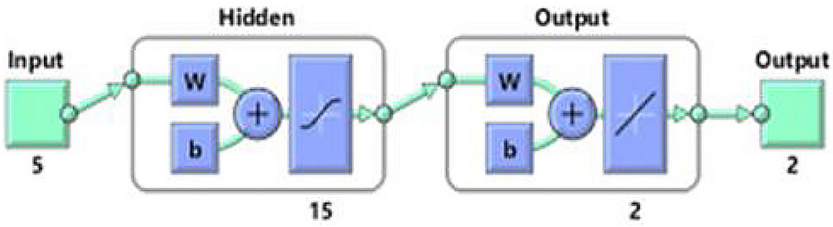

Figure 4. ANN architecture implemented structure

determine the optimal level of parameters to use to maximize tensile strength and minimize roughness of the surface. Statistical ANOVA also calculated the relative values of each parameter and how they interact to contribute to these measures of performance. Table 3 shows that tensile strength increased from 26.51 MPa to 38.46 MPa when the specimens were printed with 0.24 mm (level 3) of layer thickness of the layer, an infill density of 80 percent (level 3), and a line infill pattern. This is important because it is beyond the 32.5 MPa maximum tensile strength as reported in the reference [38]. On the other hand, the surface roughness was reduced to 4.83 μm and 1.88 μm using a layer thickness of 0.16 mm (level 1), an infill density of 60 (level 2), and a grid infill pattern (level 2). ANOVA of the data in Table 3 has determined the important parameters and interactions that affect the maximization of tensile strength and minimization of surface roughness, with the findings being summarized in Table 4.

For UTS, all factors are significant ($p < 0.05$): infill pattern (C) contributes most (38.1%, F=8.01), then density (B, 29%, F=7.73), then thickness (A, 20.1%, F=6.86) with an error of 4.4%. In the case of Ra, thickness (A) prevails (47.4, F=16.24, p=0.010), density (B), next (34.41, F=10.43, p=0.023), and pattern (C), smallest (15.38, F=2.20, p=0.198), error 1.91%. Optimized settings included in Table 5 are 0.24 mm thickness, 80% density, Line pattern to achieve the highest UTS; 0.2 mm thickness, 60% density, Grid pattern to achieve the lowest Ra. respectively, which are shown in Figure 5(a) and 5(b). The performance of line infill is better than others in UTS because of its continuous and aligned structure, which reduces the

Table 3. Tensile strength and surface roughness: Experimental results

Exp. No.	Layer thickness (mm)	Infill density (%)	Infill pattern	Ultimate tensile stress UTS (MPa)	Surface roughness Ra (μm)
1	0.16	40	Gyroid	32.891	3.52
2	0.16	40	Grid	35.486	3.64
3	0.16	40	Line	32.653	3.74
4	0.16	60	Gyroid	33.924	2.81
5	0.16	60	Grid	31.84	**1.88**
6	0.16	60	Line	29.202	2.61
7	0.16	80	Gyroid	33.67	2.62
8	0.16	80	Grid	29.452	2.14
9	0.16	80	Line	37.482	2.15
10	0.2	40	Gyroid	31.561	2.81
11	0.2	40	Grid	31.972	3.02
12	0.2	40	Line	31.717	3.02
13	0.2	60	Gyroid	32.36	3.18
14	0.2	60	Grid	**26.508**	2.76
15	0.2	60	Line	28.261	2.89
16	0.2	80	Gyroid	34.241	3.8
17	0.2	80	Grid	26.755	2.55
18	0.2	80	Line	37.348	2.74
19	0.24	40	Gyroid	34.097	3.22
20	0.24	40	Grid	31.001	3.24
21	0.24	40	Line	34.273	3.21
22	0.24	60	Gyroid	34.17	3.91
23	0.24	60	Grid	26.562	3.32
24	0.24	60	Line	31.28	2.98
25	0.24	80	Gyroid	34.165	**4.8**3
26	0.24	80	Grid	26.328	3.77
27	0.24	80	Line	**38.463**	3.69

Table 4. ANOVA tensile strength and surface roughness results

ANOVA for tensile strength						
Source	DF	Adj SS	Adj MS	F-Value	P-Value	Percentage contribution
A	1	5.3247	5.3247	6.86	0.023	20.1
B	1	7.6790	7.6790	7.73	0.038	29
C	1	10.083	10.083	8.01	0.043	38.1
Error	5	1.6473	0.2295			4.4
Pure Error	2	0.4627	0.2313			1.7
Total	14	26.5206				
ANOVA for surface roughness						
Source	DF	Adj SS	Adj MS	F-Value	P-Value	Percentage contribution
A	1	9.8076	9.8076	16.24	0.010	47.4
B	1	7.1322	7.1322	10.43	0.023	34.41
C	1	3. 178	3. 178	2.20	0.198	15.38
Error	5	0.3948	0.08896			1.91
Pure Error	2	0.4864	0.18363			2.33
Total	14	20.683				100

Table 5. The ideal values and significance for every parameter

Parameters	Layer thickness (LT)	Infill density (ID)	Infill pattern (IP)	Significant
Optimized UTs	0.24	80	Line	Infill pattern (%)
Optimized Ra	0.16	60	Grid	Layer thickness (mm)

stress concentration at intersections (in comparison with grid/Gyroid), making it possible to transfer loads efficiently and achieve stronger interlayer bonding. Thicker (0.24 mm) layers increase UTS through increased contact and diffusion time to form strong bonds, whereas thinner (0.2 mm) layers decrease Ra through finer resolution, yet weaken bonds due to quick cooling and smaller necks [39]. These trends are due to the fact that the infill patterns make TPU 3D-printed components more resistant to tensile stresses by raising internal structural density and load distribution, forming more interconnected lattices that are more resistant to uniaxial forces. Dense infills reduce stress concentration at void boundaries, seen in finite element analysis, and the thickness of the layer is the primary contributor to the roughness of surfaces, with layers of greater thickness enhancing the stair-stepping effect of stacking layers and the Ra value; whereas thin layers enhance interlayer fusion and nice, which reduces the number of cusps visible. The contribution percentage of each parameter measures the contribution it makes to the overall change in results. The infill pattern affected the tensile strength (UTS) most (38.1%), then infill density (29%), and layer thickness (20.1%). In the case of surface roughness (ra), the layer thickness prevailed (47.4%), infill density (34.41%), and lastly, infill pattern had the least impact (15.38%, $p = 0.198 > 0.05$). The best settings were summarized in Table 5: 0.24 mm layer thickness, 80% infill density, and Line pattern to maximize UTS; 0.16 mm layer thickness, 60% infill density, and Grid pattern to minimize (Ra).

Results of ANN model

The predictive models based on artificial neural networks (ANNs) were trained on the experimental data, which was divided in terms of the epoch to ensure that comparisons could be made with experimental data; the sample output is shown in Table 6, Figures 6 and 7 indicates that the lowest mean absolute error of 0.011355 was attained with epoch 0; the training, testing, and validation data were 70 percent, 15 percent,

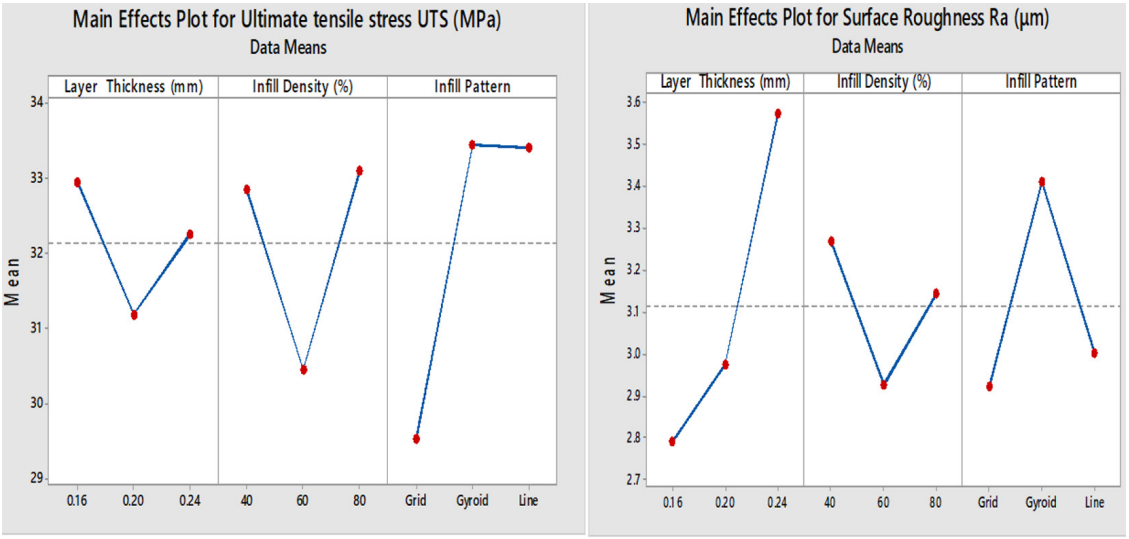

(a) (b)

Figure 5. Main effect plot for (a) tensile strength, (b) surface roughness

Table 6. Comparison of experimental values versus RSM and ANN models

No.	UTs (MPa) actual	RSM		ANN		Ra (µm) actual	RSM		ANN	
		Predicted UTs	%Error	Predicted UTs	%Error		Predicted Ra	%Error	Predicted Ra	%Error
1	32.891	33.85	2.93	32.71	0.54	3.52	3.35	4.71	3.55	4.67
2	35.486	35.65	0.49	35.56	0.21	3.64	3.41	6.27	3.51	6.49
3	32.653	31.49	3.53	31.60	3.23	3.74	3.73	0.19	3.74	0.19
4	33.924	31.92	5.90	32.84	3.19	2.81	2.80	0.42	3.70	0.32
5	31.84	30.48	4.25	30.79	3.31	2.14	2.28	6.52	2.18	6.40
6	29.202	31.42	7.60	31.22	6.90	2.61	2.66	2.00	2.61	2.00
7	33.67	35.02	4.03	34.13	1.36	2.62	2.77	5.57	2.69	1.94
8	29.452	30.34	3.05	30.15	2.37	2.14	2.21	2.05	2.51	2.14
9	37.482	36.38	2.94	36.78	1.87	2.15	2.11	1.64	2.12	1.66
10	31.561	32.76	3.80	32.16	1.90	3.21	3.09	3.79	3.19	3.82
11	31.972	32.09	0.38	31.68	0.11	3.02	3.14	4.07	3.04	4.04
12	31.717	30.86	2.69	30.98	2.32	3.02	3.20	5.81	3.10	5.67
13	32.36	30.82	4.73	31.93	1.33	3.18	3.11	2.20	3.14	2.23
14	26.508	26.92	1.56	26.62	0.43	2.76	2.59	6.24	2.69	6.41
15	28.261	30.78	5.21	30.89	5.55	2.89	2.70	6.50	2.63	4.84
16	34.241	33.93	0.89	34.14	0.31	3.8	3.66	3.82	3.77	3.85
17	26.755	26.78	0.12	26.69	0.26	2.55	2.56	0.24	2.56	0.24
18	37.348	35.741	4.29	36.85	1.34	2.74	2.73	0.28	2.63	0.30
19	34.097	34.50	1.18	34.70	1.77	3.22	3.20	0.54	3.21	0.55
20	31.001	31.36	1.16	31.12	0.39	3.24	3.25	0.42	3.23	0.42
21	34.273	33.052	3.55	33.86	1.21	3.21	3.04	5.36	3.14	5.48
22	34.17	32.57	4.68	32.77	4.10	3.91	3.80	2.77	3.81	2.84
23	26.562	26.18	1.40	26.39	0.65	3.32	3.28	1.32	3.30	1.33
24	31.28	32.98	5.44	32.18	2.88	2.98	3.12	4.77	3.03	4.69
25	34.165	35.67	4.43	35.18	2.97	4.83	4.92	1.95	4.98	1.89
26	26.328	26.056	1.03	26.16	0.65	3.77	3.82	1.38	3.72	1.40
27	38.463	37.94	1.35	38.12	0.88	3.69	3.73	1.08	3.63	1.09

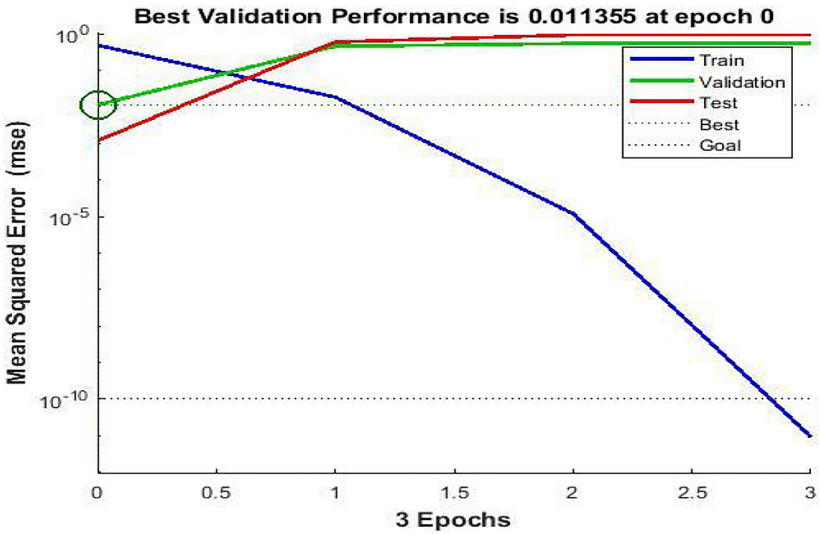

Figure 6. Tensile and surface roughness performance plot

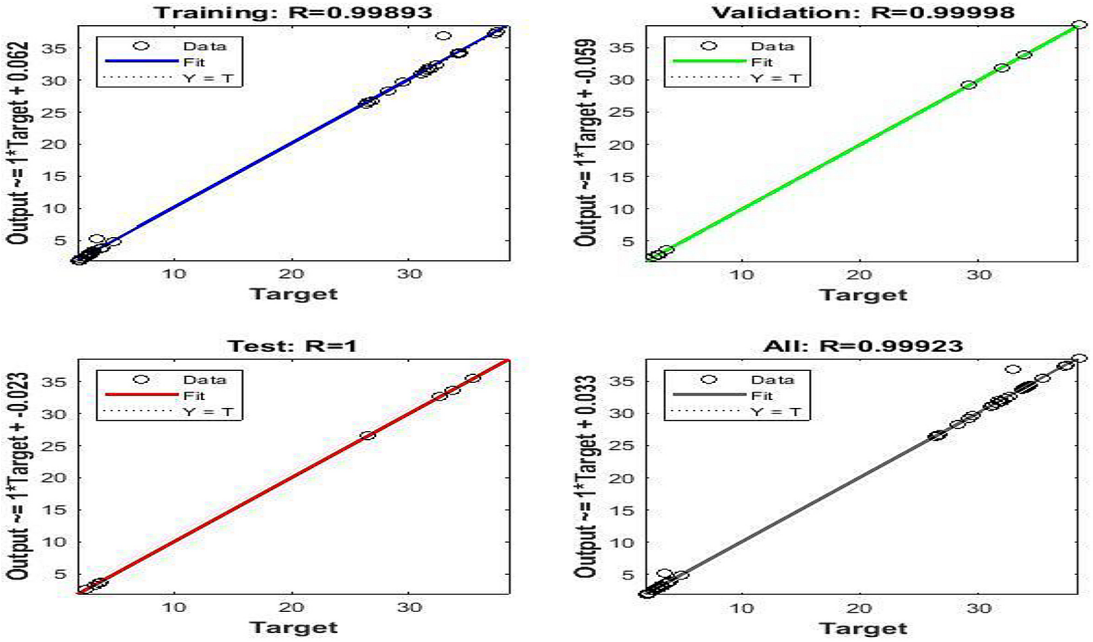

Figure 7. The proposed network graphical representation

and 15 percent respectively. The 70/15/15 (70% train, 15% validation, 15% test) tradeoff between sufficient training data and trustworthy evaluation is typical of mid-sized datasets, to focus on model evaluation rather than raw training volumes [40].

The Levenberg-Marquardt algorithm has performed the most highly in terms of performance with a correlation coefficient (R) of 0.99997 (Figure 7). It is interesting to note that the validation dataset showed the ideal regression coefficient of 1, which implies a very high correlation of ANN predictions and experimental results.

Results of RSM model

Based on the analysis of the response surface methodology (RSM) model, Equations 5 and 6 provide quadratic mathematical models of the interaction between input variables and responses to tensile strength and roughness of the surface. Such equations include linear, quadratic, and interaction terms in order to measure the total response effects that can be important predictive as well as optimization tools that can be used to see the effects of individual parameters and their combinations on system performance.

$$Tensile\ Strength\ (\text{MPa}) 113.3 - 454 \times \\ \times LT - 0.697 \times ID - 19.85 \times IP + 1163 \times \\ \times LT^2 + 0.00574 \times ID^2 + 4.331 \times IP^2 - \\ - 0.31 \times LT \times ID - 0.6 \times LT \times \\ \times IP + 0.0380 \times ID \times IP \quad (5)$$

$$Surface\ Roughness\ (\mu\text{m})\ 13.97 - 2.3 \times \\ \times LT - 0.1861 \times ID + 0.121 \times IP + 75.7 \times \\ \times LT^2 + 0.000544 \times ID^2 + 0.2211 \times \\ \times IP^2 + 0.7187 \times LT \times ID - 1.500 \times \\ \times LT \times IP - 0.01404 \times ID \times IP \quad (6)$$

Comparative proposed predictive models

To compare the prediction performance of two different methods, the findings of 27 experiments which were performed according to Taguchi L27 design were used. The two ANN and RSM methods were used to predict the ultimate tensile strength (UTS) and surface roughness (Ra) values, which are the two output responses of the experiments, A statistical comparison was made to compare the RSM and ANN models alongside the use of Equation 7.

$$Error\ \% = |((Measured\ value - Predicted\ value)/ \\ (Measured\ value))| \times 100 \quad (7)$$

Table 6 shows the comparison between actual and predicted UTS and Ra. demonstrate ANN had better accuracy, with a tensile strength prediction error is 6.90% and a surface roughness prediction error is 6.49%. Comparatively, tensile strength and surface roughness errors in the RSM model were 7.60 and 6.50, respectively. Also, ANN had a lower error rate whereby the mean absolute error (MAE) of UTS prediction was 0.011. Conversely, the MAE of RSM was determined to be 0.54. On the same note, ANN showed better results in the prediction of Ra with a value of 0.032 as compared to this being calculated to be 0.16 with RSM. ANN generated a curve nearer to the experimental results in both UTS prediction and Ra prediction, and RSM showed larger deviation of the experimental results. According to these findings, ANN is a more efficient model in estimating the two-performance metrics. Concerning the analysis of standard error, the findings also confirm better performance of ANN. In the case of UTS predictions, ANN gave more reliable output with less variations against actual values particularly at the peaks (around experiment number 26–27). ANN prediction error bands were considerably smaller than RSM and this indicates that it is a more reliable predictor. Similarly, with ANN, the standard errors were smaller in all experimental range, especially in the regions of rapid change (experiments 5–8). RSM demonstrated a wider pattern of standard error bands and thus, higher levels of prediction uncertainty particularly when the value is at the extreme levels. This regular trend of reduced standard errors in ANN predictions of the two properties highlights its statistical strength and validity as a prediction instrument. The standard consistency in the performance of standard errors with both UTS and Ra predictions indicates that ANN provides more reliable and accurate estimates of the printed part traits. The ANN and RSM models were tested using validation to confirm that they were accurate predictors. Table 6 along with Figures 8 and 9 compares the predictive success of ANN and RSM to UTS and Ra when applied to defined conditions of input. The table displays the percentage of errors

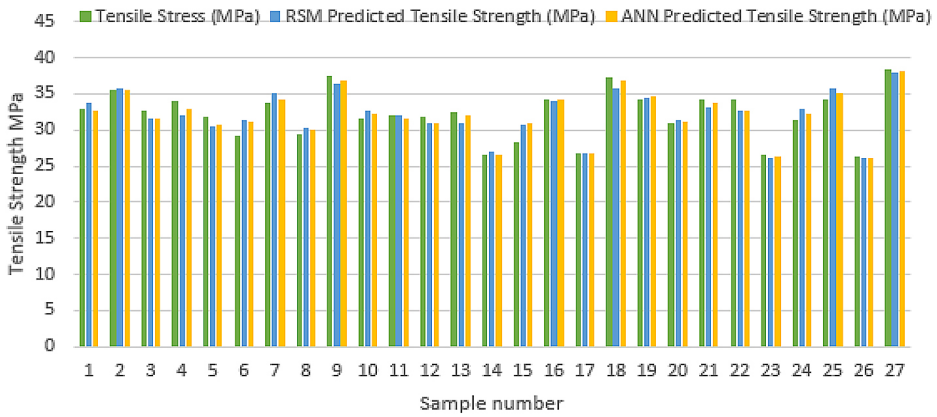

Figure 8. Experimental vs ANN and RSM predicted tensile strength value

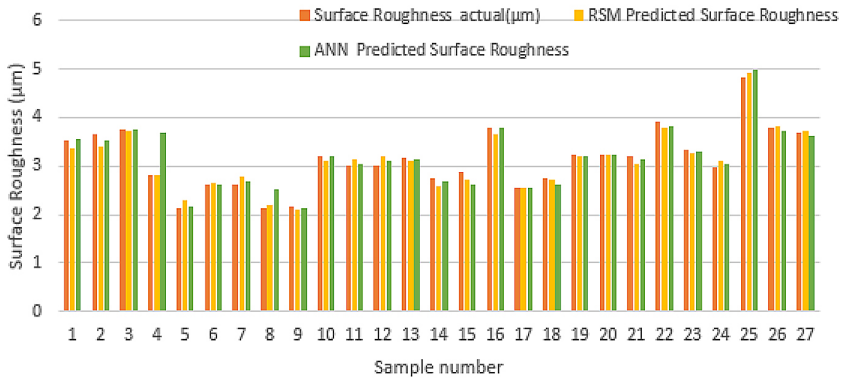

Figure 9. Experimental vs ANN and RSM predicted surface roughness value

between the actual and predicted values in different experimental conditions. The average error in UTS of ANN is very low and generally is between 0.21–3.23%. This illustrates the high ability of ANN in UTS prediction. On the other hand, the percentage of errors in RSM is larger with a range of 0.49 to 7.60. A similar situation exists with Ra, with ANN having an average error of 1.36, when compared to RSM, which has 2.37. The low error rates associated with the predictive performance of ANN demonstrate the fact that it is able to determine the input-output relationships better. In general, the average error rate of ANN is about 0.80% with UTS and 1.51 with Ra, which is higher compared to the average rates of 3.19% and 2.85 with RSM. The above results make it clear that ANN produces more accurate and reliable predictions compared to RSM with particularly high performance when dealing with nonlinear and complex datasets.

CONCLUSIONS

In the present research, TPU samples were fabricated using FDM, a flexible AM method appreciated for its affordability, simplicity, and versatility with soft materials. The effects of layer thickness, infill density, and infill pattern on the output parameters (i.e., UTS and Ra) of FDM printing of TPU have been investigated both experimentally and through predictive modeling. The Taguchi L27 and ANN, RSM-based techniques were used to define the best printing parameters for printing quality parts. The main results of this paper may be reduced as follows:

- Pattern of infill was found to have the greatest contribution towards UTS (38.1% contribution, p=0.043). UTS was maximized at 80 percent infill density, which was the line pattern. UTS rose as the layer thickness (0.24 mm optimum) increased.
- Layer thickness was established to have the greatest effect on Ra (47.4% contribution, p=0.010). The minimum thickness of the ra was 0.20 mm using a grid. The density of the infill that reduced the ra was moderate (60%), whereas the pattern had the least influence (15.38%).
- It was established that ANN is better than RSM in terms of prediction accuracy (max errors 6.90% UTS and 6.49% Ra), reduced MSE (0.80 UTS, 1.51 Ra), and R=0.99997.
- ANOVA optimum parameters were LT 0.24 mm, ID 80, IP Line (maximum UTS) 38.463 Mpa, and LT 0.20 mm, ID 60, IP Grid (minimum Ra) 1.88 u m.
- ANN model validation demonstrated MAE 0.011 (UTS) and 0.032 (Ra) in 27 experiments, which indicated that ANN models are more stable in predicting all conditions than RSM.
- Analysis of standard errors established that ANN predicts narrower bands as compared to RSM, especially more accurate at extreme parameter values (experiments 26-27 of UTS and 5-8 of Ra).

The best FDM parameters obtained through Taguchi/RSM/ANN in the printing process of TPU are a good reference for manufacturing operators. Application of these parameters may result in improved performance of the mechanics and the quality of the surface, as well as the decreased number of repeated experiments. These results can be used in the optimization of additive manufacturing, providing a realistic set of guidelines that can be used to create high-performance flexible TPU components.

REFERENCES

1. Ligon SC, Liska R, Stampfl J, Gurr M, Mülhaupt R. Polymers for 3D printing and customized additive manufacturing. Chemical reviews. 2017 Aug 9;117(15):10212–90. https://doi.org/10.1021/acs.chemrev.7b00074
2. Steenhuis HJ, Pretorius L. The additive manufacturing innovation: a range of implications. Journal of Manufacturing Technology Management. 2017 Feb 6;28(1):122–43. https://doi.org/10.1108/JMTM-06-2016-0081
3. Kafle A, Luis E, Silwal R, Pan HM, Shrestha PL, Bastola AK. 3D/4D printing of polymers: fused deposition modelling (FDM), selective laser sintering (SLS), and stereolithography (SLA). Polymers. 2021 Sep 15;13(18):3101. https://doi.org/10.3390/polym13183101
4. Rosato DV, Rosato DV, Rosato MG. Molding materials. InInjection Molding Handbook 2000 (pp. 479–622). Boston, MA: Springer US. https://doi.org/10.1007/978- 1-4615-4597-2_6
5. Shaqour B, Abuabiah M, Abdel-Fattah S, Juaidi A, Abdallah R, Abuzaina W, Qarout M, Verleije B, Cos P. Gaining a better understanding of the extrusion process in fused filament fabrication 3D printing: A review. The International Journal of Advanced Manufacturing Technology. 2021 May;114(5):1279–91. https://doi.org/10.1007/s00170-021-06918-6
6. Hanft D, Exner J, Schubert M, Stöcker T, Fuierer P, Moos R. An overview of the aerosol deposition method: Process fundamentals and new trends in materials applications. J. Ceram. Sci. Technol. 2015 Sep 1;6(3):147–82. https://doi.org/10.4416/JCST2015-00018
7. Ameen AA, Takhakh AM, Abdal-Hay A. Mechanical compressive properties of TPU 3D printed with various parameters. Al-Qadisiyah J. Eng. Sci. 2024;17:371–82. https://doi.org/10.30772/qjes.2024.148664.1193
8. Yadavalli VR, Myadam AK, Telu SB. FDM 3D-Print on thermoplastic polyurethane (TPU) with different process parameters using gyroid and zigzag infill patterns. Open Access Libr. J. 2024;11:e11203. https://doi.org/10.4236/oalib.1111203
9. jakab sk, lendvai l. effect of printing parameters on the tensile mechanical properties of 3d-printed thermoplastic polyurethane. Engineering Proceedings. 2025 Oct 29;113(1):19. https://doi.org/10.3390/engproc2025113019
10. Salbiah UK, Shieddique AD, Rohman R. Optimizing process Parameters for Filament 3d Printing using Thermoplastic Polyurethane (tpu) with Response Surface Methodology (rsm). Media Mesin: Majalah Teknik Mesin. 2025 Jul 31;26(2):59–70. https://doi.org/10.23917/mesin.v26i2.4771
11. Albardawil A, Aditya AR, Mubarok MY, Islami LA, Mardiyana D. Improving the mechanical performance of TPU95A filament in FDM 3D printing via parameter optimization using the Taguchi method. Engineering Proceedings. 2025 Sep 4;107(1):62. https://doi.org/10.3390/engproc2025107062
12. Elmrabet N, Siegkas P. Dimensional considerations on the mechanical properties of 3D printed polymer parts. Polymer Testing. 2020 Oct 1;90:106656. https://doi.org/10.1016/j.polymertesting.2020.106656
13. Wang J, Yang B, Lin X, Gao L, Liu T, Lu Y, Wang R. Research of TPU materials for 3D printing aiming at non-pneumatic tires by FDM method. Polymers. 2020 Oct 27;12(11):2492. https://doi.org/10.3390/polym12112492
14. Fallahiarezoudar E, Ngadiman NH, Yusof NM, Idris A, Ishak MS. Development of 3D thermoplastic polyurethane (TPU)/Maghemite (Υ-Fe_2O_3) using ultra-hard and tough (UHT) bio-resin for soft tissue engineering. Polymers. 2022 Jun 23;14(13):2561. https://doi.org/10.3390/polym14132561
15. Ferretti P, Leon-Cardenas C, Sali M, Santi GM, Frizziero L, Donnici G, Liverani A. Application of TPU—Sourced 3D printed FDM organs for improving the realism in surgical planning and training. InProceedings of the 11th Annual International Conference on Industrial Engineering and Operations Management, Singapore 2021 Mar 7 (pp. 7–11). https://doi.org/10.46254/AN11.20211136
16. Soykan U. Production of TPU-reinforced 3D printing PLA filaments: Structural, phase transition and crystallinity properties. International Journal of Advances in Engineering and Pure Sciences. 2025;37(3):224–30. https://doi.org/10.7240/jeps.1674753
17. Ursini C, Collini L. FDM layering deposition effects on mechanical response of TPU lattice structures. Materials. 2021 Sep 28;14(19):5645. https://doi.org/10.3390/ma14195645
18. Haryńska A, Carayon I, Kosmela P, Brillowska-Dąbrowska A, Łapiński M, Kucińska-Lipka J, Janik H. Processing of polyester-urethane filament and characterization of FFF 3D printed elastic porous structures with potential in cancellous bone tissue engineering. Materials. 2020 Oct 8;13(19):4457. https://doi.org/10.3390/ma13194457
19. Rodríguez L, Naya G, Bienvenido R. Study for the selection of 3D printing parameters for the design of TPU products. InIOP Conference Series: Materials Science and Engineering 2021 Oct (Vol. 1193, No. 1, p. 012035). IOP Publishing. https://doi.org/10.1088/1757-899X/1193/1/012035
20. Kumar S, Singh I, R. Koloor SS, Kumar D, Yahya MY. On laminated object manufactured FDM-printed ABS/TPU multimaterial specimens: an insight into mechanical and morphological characteristics.

Polymers. 2022 Sep 28;14(19):4066. https://doi.org/10.3390/polym14194066

21. Marco V, Massimo G, Manuela G. Additive manufacturing of flexible thermoplastic polyurethane (TPU): enhancing the material elongation through process optimisation. Progress in Additive Manufacturing. 2025 Apr;10(4):2877–91. https://doi.org/10.1007/s40964-024-00790-y
22. Kulkarni A, Eckey L, Mosca P, Chaudhary R, Hadian A, Pearce JM, Clemens F, Soraru GD. Effect of thermoplastic polyurethane filament on the cellular ceramics structures obtained from material extrusion and polymer-derived ceramic. Progress in Additive Manufacturing. 2025 Nov;10(11):10331–42. https://doi.org/10.1007/s40964-025-01243-w
23. Dey A, Yodo N. A systematic survey of FDM process parameter optimization and their influence on part characteristics. Journal of Manufacturing and Materials Processing. 2019 Jul 29;3(3):64. https://doi.org/10.3390/jmmp3030064
24. Sheoran AJ, Kumar H. Fused Deposition modeling process parameters optimization and effect on mechanical properties and part quality: Review and reflection on present research. Materials Today: Proceedings. 2020 Jan 1;21:1659–72. https://doi.org/10.1016/j.matpr.2019.11.296
25. Solomon IJ, Sevvel P, Gunasekaran JJ. A review on the various processing parameters in FDM. Materials Today: Proceedings. 2021 Jan 1;37:509–14. https://doi.org/10.1016/j.matpr.2020.05.484
26. Cerda-Avila SN, Medellín-Castillo HI, Lim T. An experimental methodology to analyse the structural behaviour of FDM parts with variable process parameters. Rapid Prototyping Journal. 2020 Sep 29;26(9):1615–25. https://doi.org/10.1108/RPJ-12-2019-0312
27. Torres J, Cole M, Owji A, DeMastry Z, Gordon AP. An approach for mechanical property optimization of fused deposition modeling with polylactic acid via design of experiments. Rapid Prototyping Journal. 2016 Mar 21;22(2):387–404. https://doi.org/10.1108/RPJ-07-2014-0083
28. Tahseen FA, Alaa HS. Path Planning Optimization of a Mobile Robot based on Intelligence Algorithm. In3rd International Conference on Sustainable Engineering Techniques (ICSET 2020), IOP Conf. Series: Materials Science and Engineering 2020;881:012047. https://doi.org/10.1088/1757-899X/881/1/012047
29. Abdullah MA, Abed AH, Mansor KK. Comparison between low-carbon steel and galvanized steel by deep drawing under the influence of different parameters. Management Systems in Production Engineering. 2025. https://doi.org/10.2478/mspe-2025-0016
30. Günay M, Yücel E. Application of Taguchi method for determining optimum surface roughness in turning of high-alloy white cast iron. Measurement. 2013 Feb 1;46(2):913–9. https://doi.org/10.1016/j.measurement.2012.10.013
31. Anderson MJ, Whitcomb PJ. RSM simplified: optimizing processes using response surface methods for design of experiments. Productivity press; 2016 Aug 5. https://doi.org/10.4324/9781482293777
32. Shabeeb AH, Abdulwahhab AB, Ismael HS, Ghazi SK. Optimization of fused deposition modeling parameters to enhance tensile strength and surface roughness of polyethylene terephthalate glycol. Advances in Science and Technology. Research Journal. 2025;19(8). https://doi.org/org/10.12913/22998624/205716
33. Ahmed, B.A., Abdullah, M.A. and Ghazi, S.K., Surface roughness of aluminum alloy 7024 predicted by linear regression and neural network model in abrasive water jet machining. Al-Bahir Journal for Engineering and Pure Sciences, 2024;4(2):7. https://doi.org/10.55810/2313-0083.1060
34. Ünal HT, Başçiftçi F. Evolutionary design of neural network architectures: a review of three decades of research. Artificial Intelligence Review. 2022 Mar;55(3):1723–802. https://doi.org/10.1007/s10462-021-10049-5
35. Ibraheem MQ, Obaeed NH, Abdulridha HH. Optimizing the MRR in WEDM process by using Taguchi analysis and GA technique. InAIP conference proceedings 2024 Jun 10 (Vol. 3002, No. 1, p. 050013). AIP Publishing LLC. https://doi.org/10.1063/5.0205987
36. Shakir LF, Ismael HS, Abdullah MA, Huayier AF, Ghazi SK. Multi-objective prediction and optimization of 3D-printed polymer properties using neural networks and desirability functions. Advances in Science and Technology Research Journal. 2026 Jan 1;20(1):288–300. https://doi.org/10.12913/22998624/210935
37. Shabeeb AH, Abdulridha HH, Obaeed NH, Mohammed MM. Multi-objective optimization and prediction of milling parameters for Al 6061 alloy using desirability analysis and artificial neural networks. Engineering Research Express. 2025 Jun 30;7(2):025528. https://doi.org/10.1088/2631-8695/add1ae
38. Jakab SK, Lendvai L. Effect of printing parameters on the tensile mechanical properties of 3D-printed thermoplastic polyurethane. Engineering Proceedings. 2025 Oct 29;113(1):19. https://doi.org/10.3390/engproc2025113019
39. Jasim MF, Huayier AF, Abbas TF. Investigation of the Effect of Surface Roughness and Dimensional Accuracy on the Layer Thickness of PLA Parts Produced by the FDM Process. InProgress in Engineering Technology V 2023 May 28 (pp. 19–29). Cham: Springer Nature Switzerland. https://doi.org/10.1007/978-3-031-29348-1_3
40. Mazumder PT. Explainable and fair anti-money laundering models using a reproducible SHAP framework for financial institutions. Discover Artificial Intelligence. 2026 Feb 22. https://doi.org/10.1007/s44163-026-00944-7